LA-UR-15-28079
Approved for public release; distribution is unlimited.

Title: The thermal conductivity of mixed fuel UxPu1-xO2: molecular dynamics simulations

Author(s): Liu, Xiang-Yang
Cooper, Michael William Donald
Stanek, Christopher Richard
Andersson, Anders David Ragnar

Intended for: Report

Issued: 2015-10-16

The thermal conductivity of mixed fuel $U_xPu_{1-x}O_2$: molecular dynamics simulations

X.-Y. Liu, M. W. D. Cooper, C. R. Stanek, D. A. Andersson
Los Alamos National Laboratory, Los Alamos, NM 87545

Mixed oxides (MOX), in the context of nuclear fuels, are a mixture of the oxides of heavy actinide elements such as uranium, plutonium and thorium [1]. The interest in the UO_2-PuO_2 system arises from the fact that these oxides are used both in fast breeder reactors (FBRs) as well as in pressurized water reactors (PWRs). The thermal conductivity of UO_2 fuel is an important material property that affects fuel performance since it is the key parameter determining the temperature distribution in the fuel, thus governing, *e.g.*, dimensional changes due to thermal expansion, fission gas release rates, *etc.* [2] For this reason it is important to understand the thermal conductivity of MOX fuel and how it differs from UO_2. Here, molecular dynamics (MD) simulations are carried out to determine quantitatively, the effect of mixing on the thermal conductivity of $U_xPu_{1-x}O_2$, as a function of PuO_2 concentrations, for a range of temperatures, 300 – 1500 K. The results will be used to develop enhanced continuum thermal conductivity models for MARMOT and BISON by INL. These models express the thermal conductivity as a function of microstructure state-variables, thus enabling thermal conductivity models with closer connection to the physical state of the fuel [3].

Computational methods

The non-equilibrium direct method [4] is employed in the MD simulations. In this method, a heat current (J) is applied to the system, and the thermal conductivity κ is computed from the time-averaged temperature gradient ($\partial T / \partial z$) from the Fourier's law,

$$\kappa = -\frac{J}{\partial T / \partial z} \quad (1)$$

The thermal conductivity calculations are carried out with the direct method as implemented in LAMMPS package [5]. All atoms in the system are initially assigned Gaussian distributed velocities. After that, the system is equilibrated for 100 ps in the

NVE ensemble so the system relaxes to the target temperature. Then, non-equilibrium MD runs are applied to the system, for a period of 13 – 26 ns. The initial 4 ns in the thermal simulation are used to accommodate the transient behavior of the system. After that, the temperature profiles are averaged over the rest of the MD time.

During MD, the hear flux between the hot and the cold regions is controlled at the desired level. The heat flux used in the simulations is 1.9 – 3.7 x 10^{-4} eV/nm^2 per time step. To fit the temperature profiles, a least-squares fit for the linear regression is used. The temperature profiles are fitted in the ranges $w < z < L_z/2 - w$, and $L_z/2 + w < z < L_z - w$, where L_z is the length of the simulation supercell in the heat flow direction, with the choice of the excluded width w as 0.13 L_z, as suggested from earlier studies [6]. The obtained gradients from the left and right slopes in the temperature profiles are then averaged to determine the thermal conductivity.

Two sets of interatomic potentials are used in this work. The first set is the Buckingham type of empirical potentials, which is used to describe the U^{4+} - O^{2-} [7], Pu^{4+} - O^{2-} [8] interactions, and O^{2-} - O^{2-} [9] interactions in $U_xPu_{1-x}O_2$. The other set is a recently developed empirical potential for UO_2, PuO_2 and their mixtures, which includes many-body effects using the embedded atom method (EAM) [10]. The MD simulations employing the EAM potential utilize a similar but slightly different procedure than described above. A detailed description of the EAM simulations can be found elsewhere [11]. For computational efficiency, the Wolf summation [12] is used to compute the long-range Coulumbic interactions for both types of potentials. The computational supercells are initially set to the optimized lattice constants, ranging from 0.5396 nm (PuO_2) to 0.5469 nm (UO_2), with L_z ranging from 25 to 66 nm. For all the simulations, the heat flow direction is in the <100> crystal direction. NPT simulations are carried out to determine the thermal expansion at different temperatures, for each randomly distributed composition of $U_xPu_{1-x}O_2$. All thermal conductivity MD simulations are carried out with thermal expansion taken into account. In the MD simulations, a fairly significant portion of phonons propagate ballistically through the system due to the significant large phonon mean free path relative to the simulation supercells, and scatter from the hot and cold plates. This causes the thermal conductivity obtained from MD simulations to be lower

than they should be, especially at low temperatures. The fitting formula used to extract the thermal conductivity for a simulation cell of infinite length is,

$$\frac{1}{\kappa} = \frac{1}{\kappa_\infty} + \frac{c_1}{L_z} + \frac{c_2}{L_z^2} \qquad (2)$$

where c_1 and c_2 are both constants, κ_∞ is the thermal conductivity for a simulation cell of infinite length. For temperatures higher than or equal to 600 K, c_2 is set to zero.

Results

In figure 1(a), the thermal conductivity of $U_xPu_{1-x}O_2$, obtained from the MD simulations using the Buckingham potential is shown. For mixed oxides, the positions of Pu ions are randomly distributed on U sites (substitutional). The MD calculated thermal conductivity for pure PuO_2 is slightly higher than that of UO_2 at 300 K, and is close to that of UO_2 at higher temperatures. However, if the spin-phonon scattering mechanism active in UO_2 is taken into account, the thermal conductivity of UO_2 is lower than for PuO_2. PuO_2 is non-magnetic and it is consequently not subjected to this mechanism. The spin-phonon scattering mechanism is not accounted for the in the following discussion, not for UO_2 or for the mixed oxides. The general conclusions are still valid. For the mixed oxide having 50% PuO_2 concentration ($U_{0.5}Pu_{0.5}O_2$), the thermal conductivity is generally smaller than either those of UO_2 or PuO_2. At 300 K, the reduction in the thermal conductivity for $U_{0.5}Pu_{0.5}O_2$ is about 3 – 6 W/Km compared to those of UO_2 or PuO_2 or 11 – 20% smaller. However, such reduction in thermal conductivity decreases as temperature is increased. At 600 K, the reduction in the thermal conductivity of $U_{0.5}Pu_{0.5}O_2$ is only about 2 W/Km compared to those of UO_2 or PuO_2, and 0.2 – 0.3 W/Km at 900 and 1500 K.

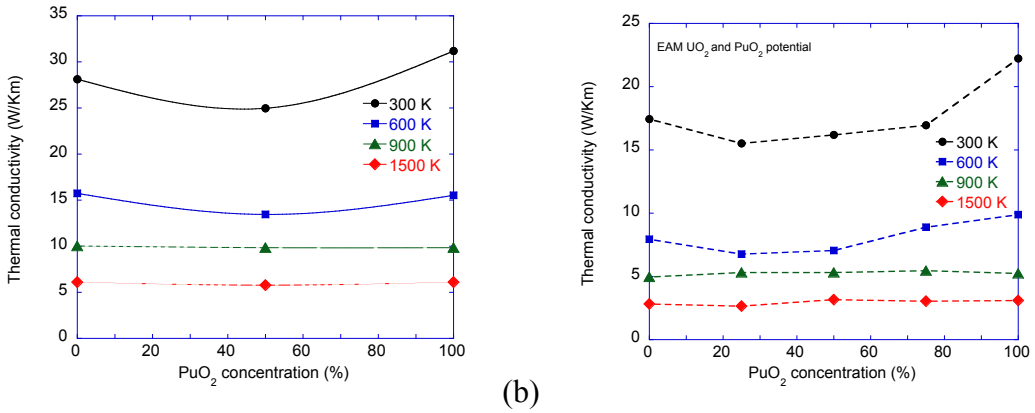

Figure 1. (a) The thermal conductivity of $U_xPu_{1-x}O_2$ calculated from MD simulations, as a function of PuO_2 concentrations at 300, 600, 900, and 1500 K, using the Buckingham potential. The solid lines are spline fit the MD data. (b) The MD determined thermal conductivity of $U_xPu_{1-x}O_2$ using the EAM potential.

In Fig. 1(b), a similar set of thermal conductivity results from MD simulations employing the EAM potential is shown. In addition to $U_{0.5}Pu_{0.5}O_2$, two additional PuO_2 concentrations, $U_{0.25}Pu_{0.75}O_2$ and $U_{0.75}Pu_{0.25}O_2$, were used in the simulations. The absolute values of the thermal conductivities determined from the MD simulations are generally smaller than in the Buckingham potential case. However, the general trend of the thermal conductivity of the mixed oxides is the same as observed in Fig. 1(a), *i.e.*, about 11% smaller than those of UO_2 at 300 K, and the reduction in the thermal conductivity becomes insignificant as the temperature increases.

The weak scattering effect in the mixed oxides can be explained through two factors (1) the small lattice constant difference between PuO_2 and UO_2, and (2) the small mass difference between U and Pu. At low temperatures, the phonon-defect scattering due to the non-uniform cation sublattice still contributes appreciably to the thermal resistence. Such scattering becomes progressively less important as phonon-phonon scattering dominates at higher temperatures.

Mixed oxide data adjusted for the spin scattering

In previous work [11] MD data for the $U_xPu_{1-x}O_2$ and $U_xTh_{1-x}O_2$ systems using the EAM potential was fitted to the following expression for $A_xB_{1-x}O_2$:

$$k = \frac{1}{xw_A + (1-x)w_B + x(1-x)C_{AB}} \quad (3)$$

where $w = A + BT$ for a particular end member and C_{AB} is the parameter relating to the strength of phonon scattering associated with the mixed cation lattice . Although, the previous work defined $C_{UPu} = 5.21 \times 10^{-2}$ mKW^{-1} and $C_{UTh} = 2.59 \times 10^{-1}$ mKW^{-1} by fitting equation 3 to MD data, they did not consider the possibility of spin scattering in the UO_2 phase, as has been done elsewhere through the Callaway model [13]. Therefore, we have combined the $A_{UO_2} = 3.11 \times 10^{-2}$ mKW^{-1} and $B_{UO_2} = 2.08 \times 10^{-4}$ mW^{-1} [13] that were adjusted for spin scattering with the previously reported C_{UPu}, C_{UTh}, A_{PuO_2}, B_{PuO_2}, A_{ThO_2} and B_{ThO_2} [11]. Figure 2 reports equation 3 as a function of temperature and composition, x.

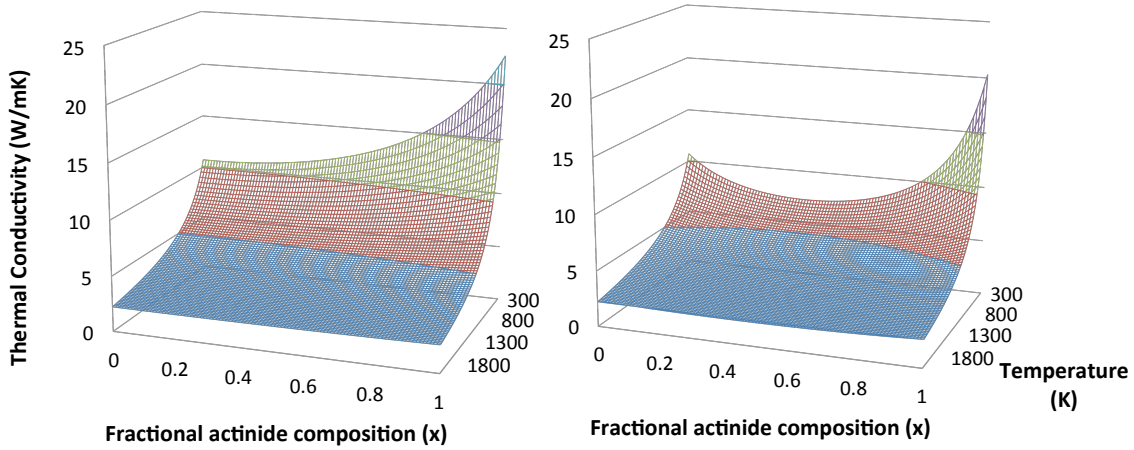

Figure 2. The thermal conductivity of (a) $U_{1-x}Pu_xO_2$ and (b) $U_{1-x}Th_xO_2$ from equation 3 parameterized using MD data from the EAM potential. The pure UO_2 parameters have adjusted to account for spin scattering in the mixed oxides [13].

For $U_{1-x}Pu_xO_2$ the inclusion of spin scattering has a dramatic effect in comparison to Figure 1. Rather than UO_2 thermal conductivity being degraded by the addition Pu it is in fact increase. This indicates that the removal of spin scattering out weights the addition of defect scattering. Conversely, the significantly greater defect scattering in $U_{1-x}Th_xO_2$ has a greater negative impact on thermal conductivity than the positive effect of removing spin scattering. Thus the $U_{1-x}Th_xO_2$ thermal conductivity reaches a minimum at around $U_{0.58}Th_{0.42}O_2$.

The relative scattering strength of spin compared to mixed cation lattice defect scattering can be most easily seen in Figure 3. Here the results of pure MD (defect scattering only) can be compared the results that only include spin scattering but do not

account for the mixed lattice, i.e. C=0 (spin scattering only). This is done for 500 K and 1000 K. The results that include both spin scattering and defect scattering from Figure 2 are also included for comparison. These results highlight that both scattering processes are imported to get an accurate description of the mixed systems. In both systems magnetic scattering is particularly important at high U content, although the effect is particularly strong for $U_{1-x}Pu_xO_2$ where the mixed cation lattice is less important than for $U_{1-x}Th_xO_2$. At higher temperatures spin scattering and defect scatter become less significant as phonon-phonon interactions begin to dominate.

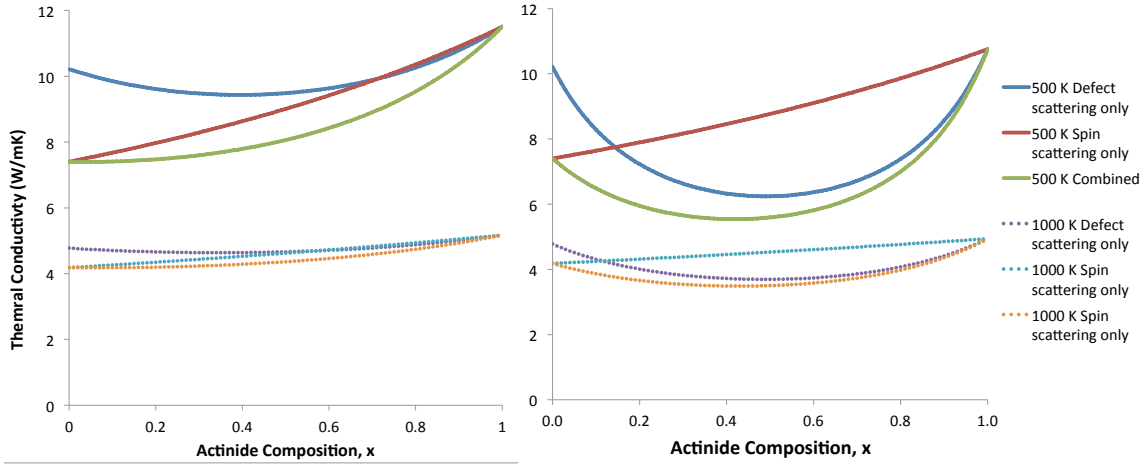

Figure 3. The different defect and spin scattering effects on the thermal conductivity of (a) $U_{1-x}Pu_xO_2$ and (b) $U_{1-x}Th_xO_2$ from equation 3 parameterized using MD data from the EAM potential at 500 K and 1000 K.

Conclusions

MD simulations have been carried out to determine quantitatively the effect of mixing on the thermal conductivity of $U_xPu_{1-x}O_2$, as a function of PuO_2 concentrations, for a range of temperatures, 300 – 1500 K. Two interatomic potentials, the Buckingham type interatomic potential and a recently developed empirical potential for UO_2, PuO_2 and their mixtures, which includes many-body effects using EAM, are used in the simulations. MD simulations using both potentials yield similar results. At 300 K, the reduction in the thermal conductivity of $U_{0.5}Pu_{0.5}O_2$ is about 10% compared to that of UO_2. Such reduction in the thermal conductivity becomes insignificant as the temperature increases. At 900 K, there is little difference in the thermal conductivity of mixed oxides and pure UO_2 or PuO_2, as obtained from MD simulations. The weak scattering effect in

the mixed oxides is presumably due to the small lattice constant and mass differences between pure UO_2 and PuO_2.

References

[1] D.A. Meneley, A.R. Dastur, P.J. Fehrenbach, Synergistic Nuclear Fuel Cycles of the Future, in, France, 1995.
[2] K. Gofryk, S. Du, C.R. Stanek, J.C. Lashley, X.Y. Liu, R.K. Schulze, J.L. Smith, D.J. Safarik, D.D. Byler, K.J. McClellan, B.P. Uberuaga, B.L. Scott, D.A. Andersson, Anisotropic thermal conductivity in uranium dioxide, Nature communications, 5 (2014).
[3] M.R. Tonks, P.C. Millett, P. Nerikar, S. Du, D. Andersson, C.R. Stanek, D. Gaston, D. Andrs, R. Williamson, Multiscale development of a fission gas thermal conductivity model: Coupling atomic, meso and continuum level simulations, Journal of Nuclear Materials, 440 (2013) 193-200.
[4] P. Jund, R. Jullien, Molecular-dynamics calculation of the thermal conductivity of vitreous silica, Physical Review B, 59 (1999) 13707-13711.
[5] http://lammps.sandia.gov.
[6] P.C. Howell, Thermal Conductivity Calculation with the Molecular Dynamics Direct Method I: More Robust Simulations of Solid Materials, J Comput Theor Nanos, 8 (2011) 2129-2143.
[7] G. Busker, A. Chroneos, R.W. Grimes, I.W. Chen, Solution mechanisms for dopant oxides in yttria, J Am Ceram Soc, 82 (1999) 1553-1559.
[8] A. Cleave, R.W. Grimes, K. Sickafus, Plutonium and uranium accommodation in pyrochlore oxides, Philos Mag, 85 (2005) 967-980.
[9] R.W. Grimes, Solution of Mgo, Cao, and Tio2, in Alpha-Al2o3, J Am Ceram Soc, 77 (1994) 378-384.
[10] M.W.D. Cooper, M.J.D. Rushton, R.W. Grimes, A many-body potential approach to modelling the thermomechanical properties of actinide oxides, Journal of Physics-Condensed Matter, 26 (2014).
[11] M. W. D. Cooper, S. C. Middleburgh, R. W. Grimes, Modelling the thermal conducitvity of $U_xTh_{1-x}O_2$ and $U_xPu_{1-x}O_2$, Journal of Nuclear Materials, 466 (2015) 29-35.
[12] D. Wolf, P. Keblinski, S.R. Phillpot, J. Eggebrecht, Exact method for the simulation of Coulombic systems by spherically truncated, pairwise r(-1) summation, J Chem Phys, 110 (1999) 8254-8282.
[13] X.-Y. Liu, M.W.D. Cooper, K. McClellan, J. Lashley, C.R. Stanek, D.A. Andersson, Thermal transport in UO_2 with defects and fission products by modelcualr dynamics, NEAMS FPL milestone report (M2MS-15LA0201031).